Electronic Supplementary Material (ESI) for Nanoscale.
This journal is © The Royal Society of Chemistry 2017

Supplementary Information:

Multi-Exciton Emission from Solitary Dopant States of Carbon Nanotubes

Xuedan Ma[1†], Nicolai F. Hartmann[1], Kirill A. Velizhanin[2], Jon K. S. Baldwin[1], Lyudmyla Adamska[2], Sergei Tretiak[1,2], Stephen K. Doorn[1], and Han Htoon[1*]

[1]Center for Integrated Nanotechnologies, Materials Physics and Applications Division,

[2]Theoretical Division, Los Alamos National Laboratory, New Mexico, 87545, USA

This document contains the following supplementary information:

SI 1. Additional Data

SI 2. Estimation of E_{11} exciton population

SI 3. Time gated 2nd order photon correlation spectroscopy

SI 4. Theoretical Model

SI 1. Additional Data

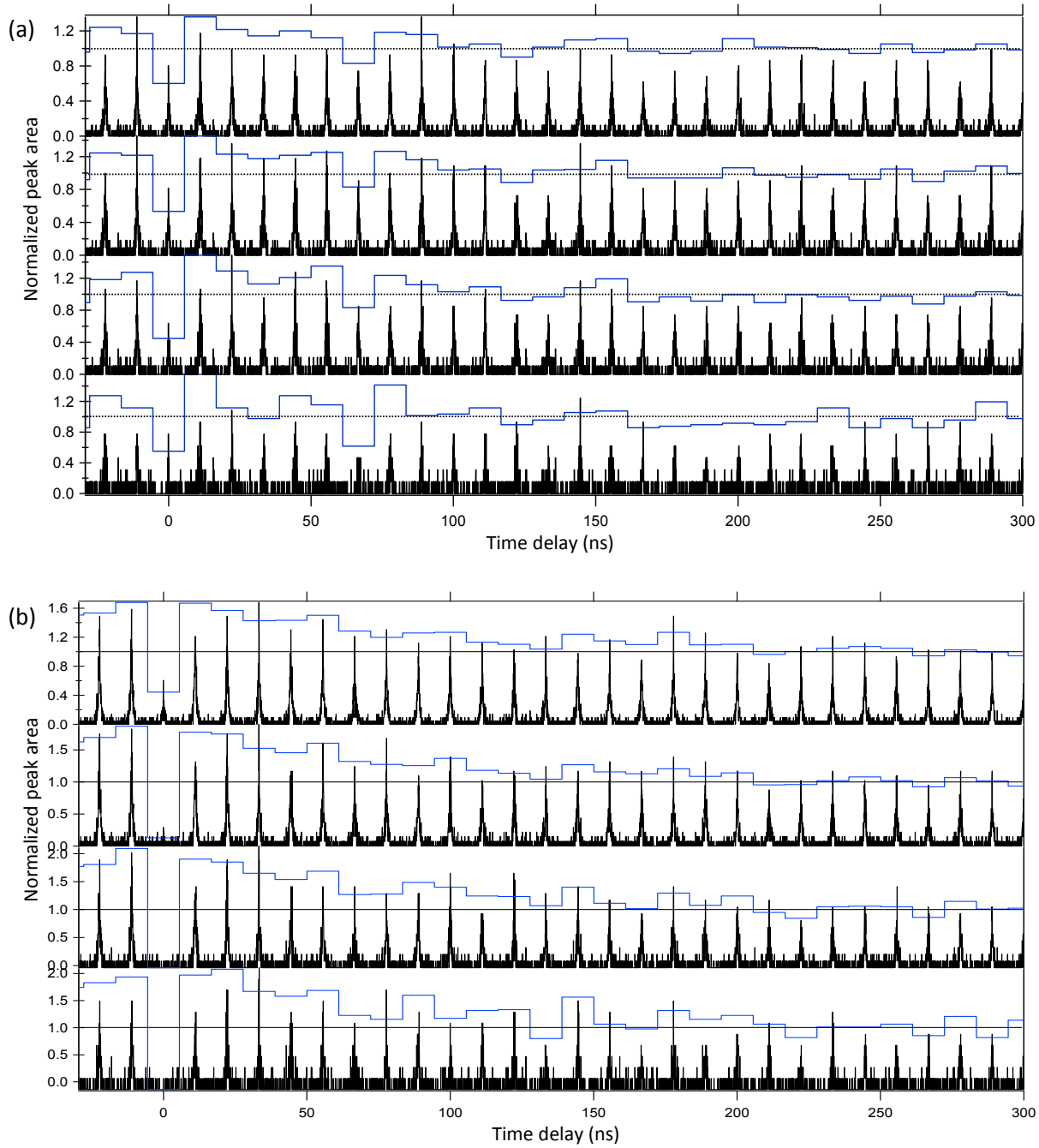

FIG. S1. $g^{(2)}$ traces of FIG. 1b (a) and 1e (b) replotted to cover time delays up to 300ns. A slight photon bunching was observed at short time delays due to PL intensity fluctuation. Blue solid lines plot the peak areas normalized by the averaged area of the peaks at time delays >175 ns. All R values are calculated using this normalization.

SI 2. Estimation of E_{11} exciton population

The number of excitons pumped into the E_{11} band is approximated by using absorption cross-section of 10^{-12} cm^2, which was recently reported in Ref. 1, 2. For excitation with a laser spot of ~ 1 μm diameter at the energy of 1.47 eV and 90 mHz repetition rate, roughly ~3 E_{11} band edge excitons are created for each 1 μW of average laser excitation power for SWCNTs with the length >1 μm. 5-20 μW pump power where $g^{(2)}$ experiments were performed and PL saturation is observed in Fig. 2 falls in 15-60 multi-exction regime. We would like to note that this number is only an estimate for an exciton population available for dopant sites, as the length of the doped nanotubes in this experiment cannot be determined precisely. Furthermore, since presence of exciton quenching sites, which compete with oxygen dopants in trapping E_{11} excitons, is known to vary widely from one tube to another, this number can only provide a qualitative indication on whether the experiment is performed in the multi-exciton regime.

SI 3. Time gated 2nd order photon correlation spectroscopy

Our time gated 2nd order photon correlation spectroscopy approach was described in detailed in Refs. 28 and 34 of the main text. Briefly, we utilized a Picoquant Hydraharp 400 multichannel picosecond event timer and TCSPC module to collect both macro-time (i.e. absolute time) and pico time (time delay between photon detection and sync pulse) of photon detection events occuring at the two detectors of the Hanbury Brown and Twiss set up simultaneously. We then post-select the photons with a picotime larger than the desired gate delay time (T_{GD}) and reconstruct the time gated $g^{(2)}$ trace using an Igor analysis routine we have developed. This approach allows us to reconstruct time gated $g^{(2)}$ traces as a function of T_{GD} from a single experiment. As the reconstructed time gated $g^{(2)}$ trace require rejection of photons detected at time delays shorter than T_{GD}, the signal to noise ratio of the $g^{(2)}$ trace reduces with the increase of $T_{GD.}$

SI 4. Theoretical Model

The exciton relaxation model for the case of no more than two excitons simultaneously present in a SWCNT is schematically depicted as a diagram in Fig. S2. Each horizontal line in the diagram represents a distinct *many-body* electronic state so that for example a state where two excitons are simultaneously present in a CNT is different, from a state where only a single exciton is present. Furthermore, since a CNT is an extended 1D object, two excitons can exist either as a non-interacting pair (when excitons are far away from each other), or, in principle, as a bound state (biexciton) – these would be two distinct many-body electronic states of different energies. The six explicitly considered electronic states of a SWCNT are (in order of decreasing energy): two free E_{11} excitons (F+F), one free E_{11} and one trapped E_{11}^{*} exciton (F+T), two trapped excitons sitting on two different dopant sites (T+T), a single free exciton (F), a single trapped exciton (T), and the ground state (i.e., no excitons) of a carbon nanotube (|g>). Whenever two excitons are present, they are assumed to form a non-interacting pair, i.e., bound biexcitons are not explicitly treated since they are assumed short-lived (see below).

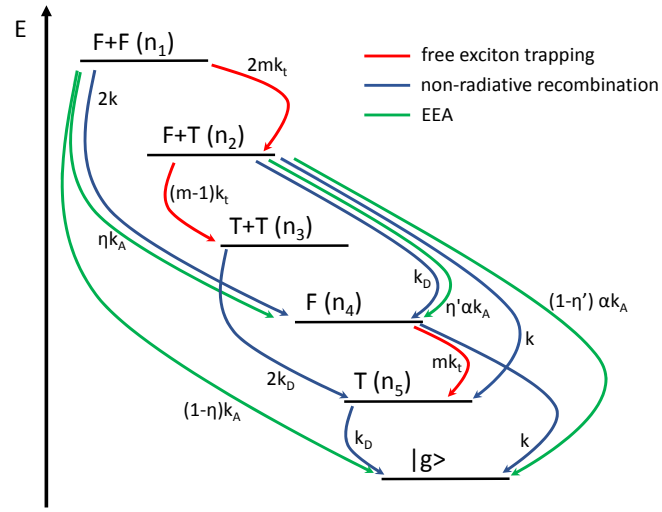

FIG. S2. Schematic diagram of proposed excitons relaxation channels. Vertical axis represents the total energy of the many-body electronic states.

Various exciton relaxation channels are shown by colored arrows in Fig. S2: trapping of a free exciton by a dopant site (red), non-radiative or radiative recombination of a free or trapped exciton (blue), and the exciton-exciton annihilation, EEA (green). Only the *energy relaxation* processes are considered and all the processes that lead to the increase of the electronic energy (except for the implicit initial photoexcitation) are neglected by assuming the limit of low temperature. Specific rate constants of elementary processes are: k_t - trapping of a free E_{11} exciton onto a dopant site, k – recombination of a free exciton radiatively or non-radiatively, k_A - EEA of the two free excitons, k_D - recombination of a trapped exciton radiatively or non-radiatively. It is assumed that the SWCNT has $m > 0$ dopant sites, so the rate constant of trapping of a free exciton to *any* of these sites is mk_t. Accordingly, the "$F + T \rightarrow T + T$" process where a single exciton already sits on a dopant site, and the other exciton is being trapped by some of the *other* $m - 1$ dopant sites, has a rate constant of $(m - 1)k_t$.

EEA of two free excitons is a complex two-stage process where two excitons, diffusing randomly along a SWCNT, first have to approach each other so that their electronic wavefunctions overlap. Once it is accomplished, the two excitons undergo a rapid Auger

recombination resulting in a single free exciton. The characteristic size of an exciton wavefunction (not the electron-hole distance, but rather a localization length of an exciton as the whole due to impurity and/or phonon-mediated scattering) was estimated to be in the range ~1.5-15 nm.[3,4] For an exciton wavefunction of this size, the time of Auger recombination can be estimated to be from a few to a few tens of femtoseconds.[5] On the other hand, the characteristic exciton diffusion times, corresponding to typical exciton diffusion lengths, can be from a few to a few hundreds of picoseconds.[3,4,6] Therefore, of the two stages of the EEA process the first – exciton diffusion – is by far the slowest, and thus the second stage – Auger recombination - can be considered instantaneous. Thus, we assign an effective rate constant k_A to the diffusion-limited EEA of two free excitons (Fig. S2), where the magnitude of this rate constant is determined by the diffusion of excitons, and not by the "intrinsic" essentially instantaneous Auger recombination.

EEA of two free excitons (F+F in Fig. S2) yields a single "hot" exciton of energy close to the E_{22} transition. A probability that this hot exciton is not lost to recombination or quenching and relaxes back to the band edge to become a free E_{11} exciton is denoted by η. Thus, there are two channels of EEA out of the F+F state with rate constants ηk_A and $(1-\eta)k_A$ corresponding to the final states of a single free E_{11} exciton or the ground state, respectively. In fact, the former channel could be strongly suppressed ($\eta \ll 1$), since for example excitons generated close to E_{22} have been observed to contribute significantly less to the band-edge PL than those generated directly at E_{11}.[7]

Now we consider a state where a single exciton is trapped by a dopant site, and the other exciton is still free (F+T state in Fig. S2). A possible relaxation channel for this state is for the second exciton to approach via diffusion the dopant site where the first exciton already sits. The two excitons can then undergo the Auger recombination. The internal structure of the exciton wavefunction (e.g., the average electron-hole distance) is not strongly affected by whether an exciton is trapped or not,[8] so we can expect the Auger recombination to be again essentially instantaneous. Therefore, F+T EEA is expected to be very similar to F+F EEA except for the fact that in the former case one of the excitons is "pinned" and does not diffuse. Accordingly, the rate constant of F+T EEA is denoted by αk_A, where α is a unitless coefficient of the order of one. For example, if we assume that the effective diffusion coefficient for F+F EEA is twice as much as for F+T EEA, because in the latter case one of the excitons is stationary, $\alpha \sim 0.5$ since $k_A \propto D$.[9] Similarly to the case of F+F EEA, we introduce η' as the probability for the F+T EEA to yield a single free exciton. Therefore, the two EEA channels for the F+T state have rate constants of $\eta' \alpha k_A$ and $(1-\eta')\alpha k_A$.

The introduced relaxation model describes at most two excitons present in a SWCNT at a time. Here we assume that if more than two free (E_{11}) excitons are initially photoexcited, they mostly annihilate each other (via F+F EEA) on a time scale much faster than the instrument response so that at most two free excitons can be realistically observed experimentally. On the other hand, if some of these free excitons become trapped before undergoing F+F EEA, the remaining free

excitons can still annihilate them (via F+T EEA). Since no more than two dopant sites per SWCNT are considered in this paper (see main text), the presence of three or more excitons in a SWCNT leads to a rapid EEA no matter excitons are trapped or not. We thus assume that whenever more than two free excitons are initially created, the relaxation dynamics of the system can be effectively described assuming the F+F state as the initial condition. This assumption is supported by the fact that the extraction of the "fast" PL lifetimes in FIG. 2(b,d) in the main text requires deconvolution of the instrument response function even at low pump powers. Therefore, the dynamics of EEA process even in the case of two excitons is already barely resolvable in the experiment.

The relaxation model described in detail above can be expressed in the form of a system of master equations, which describe the population transfer dynamics between free and dopant-trapped exciton states:

$$\frac{dn_1}{dt} = -\left(2k + 2mk_t + k_A\right)n_1, \tag{S1}$$

$$\frac{dn_2}{dt} = 2mk_t n_1 - \left(\alpha k_A + (m-1)k_t + k + k_D\right)n_2, \tag{S2}$$

$$\frac{dn_3}{dt} = (m-1)k_t n_2 - 2k_D n_3, \tag{S3}$$

$$\frac{dn_4}{dt} = \left(2k + \eta k_A\right)n_1 + \left(\eta' \alpha k_A + k_D\right)n_2 - \left(k + mk_t\right)n_4, \tag{S4}$$

$$\frac{dn_5}{dt} = kn_2 + 2k_D n_3 + mk_t n_4 - k_D n_5, \tag{S5}$$

where the correspondence between time-dependent state population, $n_i\ (i = 1,2,..,5)$, and the actual state names, e.g., F+T, are shown in Fig. S2. Calculating the time-dependent population of the ground state is not required since it does not contribute to any observables. Since only relaxation (i.e., "downhill") processes are considered, this system of five master equations, Eqs. (S1)-(S5), can in principle be solved analytically exactly, yielding five linearly independent solutions. A specific solution is found as a linear combination of these five to satisfy particular initial conditions.

Photoluminescence (PL). Within the assumed kinetic model, Eqs. (S1-S5), the time-resolved PL intensity can be written as

$$I(t) = \sum_{n=1}^{\infty} p_n I_n(t), \tag{S6}$$

where $p_n = \frac{f^n}{n!} e^{-f}$ is the Poissonian probability to initially photoexcite exactly n free excitons in a SWCNT, f being the average number of photogenerated excitons. The time-resolved PL intensity resulting from a photoexcitation of exactly n initially created free excitons is denoted by $I_n(t)$. As discussed above, we assume that if more than two excitons are created initially in a SWCNT, they quickly "die out" via EEA so that $I_n(t) \cong I_2(t)$ for $n > 2$. Accordingly, Eq. (S6) can be rewritten as

$$I(t) = p_1 I_1(t) + \tilde{p}_2 I_2(t), \tag{S7}$$

where $\tilde{p}_2 = \sum_{n=2}^{\infty} p_n = 1 - p_0 - p_1 = 1 - (1+f)e^{-f}$ is the probability of the initial photogeneration of more than a single free exciton. As expected, in the limiting case of low f one has $\tilde{p}_2 \cong p_2 \cong f^2/2$. Probability to excite more than a single exciton, $\tilde{p}_2$, becomes 50% at $f \cong 1.68$. PL intensities $I_1(t)$ and $I_2(t)$ can be obtained by solving Eqs. (S1)-(S5). Specifically, the PL intensity resulting from a photoexcitation of exactly one free exciton is

$$I_1(t) = Q_D k_D n_5^{(4)}(t), \tag{S8}$$

Here, $n_i^{(p)}(t)$ denotes $n_i(t)$ obtained by solving master equations (S1)-(S5) with the following initial condition: the population n_p is set to one at $t = 0$, and all the other populations are set to zero. For example, $n_5^{(4)}(t)$ is the time-dependent population of the single trapped exciton state, found assuming that at $t = 0$ the population of the single free exciton state was set to one, and all the other states were unpopulated. PL quantum yield of the trapped exciton is denoted by Q_D. Similarly, the PL intensity resulting from an initially photoexcited pair of excitons is

$$I_2(t) = Q_D k_D \left[n_2^{(1)}(t) + 2n_3^{(1)}(t) + n_5^{(1)}(t) \right]. \tag{S9}$$

The general expressions for $I_1(t)$ and $I_2(t)$ can be obtained exactly in a closed analytical form, e.g., in Mathematica. Simplified approximate forms of these expressions read as

$$I_1(t) \approx Q_D k_D A_1 e^{-k_D t}, \tag{S10}$$

$$I_2(t) \approx Q_D k_D \left[A_2 e^{-k_D t} + B_2 e^{-(k_F + \alpha k_A - k_t)t} \right], \tag{S11}$$

where we discarded some of the faster decaying terms since they cannot be time-resolved experimentally. The inverse lifetime of a single isolated free exciton in a SWCNT in the presence of m dopant sites is denoted by $k_F = k + mk_t$. The term $B_2 e^{-(k_F + \alpha k_A - k_t)t}$ in Eq. (S11) is actually a combination of two terms with similar decay rates – we combined them into a single effective term since they cannot be time-resolved separately. The effective rate constant $k_F + \alpha k_A - k_t$ is on the order of rate constants corresponding to diffusion-limited processes (k,k_t,k_A), i.e., it is expected to be much larger than k_D. Coefficients A_1, A_2 and B_2 are still generally too complex to be provided explicitly here. In a very specific limiting case: vanishing k_D, $m = 1$ (only a single dopant site is present in a SWCNT), $\eta = \eta' = 0$ (an EEA event results in a total loss of subsequent PL), and $\alpha = 1/2$, one has

$$A_1 = \frac{k_t}{k_F}, \tag{S12}$$

$$A_2 = \frac{2kk_t(2k + k_A + 2k_F)}{k_F(2k + k_A)(k_A + 2k_F)}, \tag{S13}$$

$$B_2 = \frac{4k_A k_t}{(2k + k_A)(2k_F + k_A + 2k_t)} - \frac{kk_t(2k + k_A)}{k_F^2(k_A + k_F)}, \tag{S14}$$

where $k_F = k + k_t$. An important observation here is that whereas A_1 and A_2 are always positive, B_2 can in principle change sign. Specifically, B_2 is positive when $k \to 0$ and all the other rate constants remain fixed. In this case, according to Eq. (S11), a bi-exponential decay can be observed in time-resolved PL. On the other hand, B_2 is negative when $k \to \infty$. In this case, the term proportional to B_2 is not a decay, but actually a *rise* which is smoothed over by the instrument response function and cannot be resolved experimentally. The physical reason for the appearance of the bi-exponential decay is that if the first exciton out of the two is trapped, its effective lifetime can be much shorter than $1/k_D$ since the second (free) exciton can still undergo F+T EEA with the first one. If, however, k is large, excitons die out radiatively or non-radiatively before they have a chance to meet each other, so that excitons are effectively non-interacting and $I_2(t)$ is effectively reduced to $I_1(t)$ with its mono-exponential decay. Thin lines in Fig. S3 show where B_2 vanishes, thus separating regions where B_2 is positive ($k \to 0$) and negative ($k \to \infty$). Solid black line corresponds to the specific case represented by Eq. (S14). Other thin lines in the same figure correspond to cases where one of the model parameters (the one shown in the legend) is changed compared to the specific case represented by Eq. (S14). As is seen, even though there is certain dependence on model parameters, the general qualitative behavior remains – B_2 is positive, and, therefore, the PL decay is bi-exponential, when k is not very large compared to k_A and k_t.

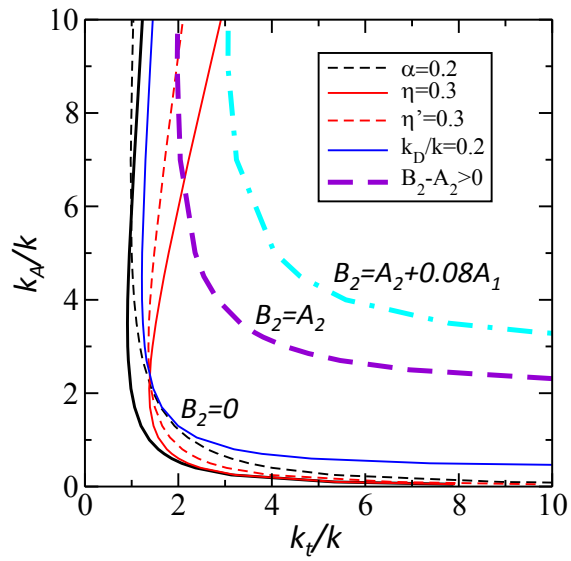

FIG. S3. Thin lines separate regions of positiveness and negativeness of coefficient B_2 in Eq. S(11), depending on the parameters of the model. Thick violet line shows where $B_2 - A_2$ changes sign.

Condition for emergence of bi-exponential decay. Since the bi-exponential decay appears in $I_2(t)$ and not in $I_1(t)$, the photon flux has to be significant, otherwise, according to Eq. (S7), the amplitude of the faster decaying component is too small to be observed experimentally. We consider a faster decaying component to be "pronounced" when its amplitude is equal or larger than the amplitude of the slow component, specifically.

$$\tilde{p}_2 B_2 \geq p_1 A_1 + \tilde{p}_2 A_2 \tag{S15}$$

As we showed above, the probability to excite at least two excitons in a SWCNT becomes more than 50% once the average number of photogenerated excitons, f, becomes larger than $\cong 1.68$. At this exciton population, however, the condition for observation of fast component can never

be met. The actual threshold for observation of the fast component is around $f \cong 2$, but at exactly $f = 2$ the observation still requires an extremely large trapping rate constant, $k_t/k > 500$. Even at relatively high exciton population of f =4, where Eq. (S15) becomes $B_2 \geq A_2 + 0.08A_1$, k_t/k and k_A/k larger than ~5 is still required (dashed cyan line of FIG. S3). On the other hand, at very high exciton populations where $\tilde{p}_2 \gg p_1$, the condition for observation of fast decay component, Eq. (S15), reduces to $B_2 \geq A_2$ and this condition can be met at k_t/k and k_A/k values of ~2 (dashed violet line of Fig. S3). In practice, we see that this regime can be realized at the average exciton population of $f \sim 10$. We expect that the condition of observation of the pronounced fast decay component can be further relaxed toward even lower k_t/k and k_A/k values if we consider higher order processes involving more than two excitons present simultaneously within a SWCNT. Indeed, as it was discussed above the physical reason for appearance of the fast decay component is that if k is small enough, then the excitons are "allowed" to interact with each other via EEA. However, the effective EEA rate constant k_A is proportional to the exciton population, so that at large exciton populations k_A can always be made larger than k, thus allowing excitons to interact, which in turn results in the appearance of the fast PL component.

Prior studies have shown that $1/k$, the decay time of the free exciton in undoped SWCNTs due to diffusion-limited quenching is in the range of 20-30 ps.[6] In a doped SWCNTs, the exciton decay time reduces down to ~8-10 ps due to diffusion-limited trapping,[6] so that $1/k_t$ could be estimated to be no less than ~10 ps, so that k_t/k is no more than ~2-3. We also expect the rate constant of the diffusion-limited EEA, k_A, to be of the same order as those of the other diffusion-processes, i.e., $1/k_A \sim 1/k_t \sim 1/k \sim$ 8-30 ps. Thus, the ratio k_A/k can only be ~ 2-3. These results lead us to the conclusion that large k_t/k and k_A/k ratios (>5-6) required for observation of fast decay component at not very high exciton populations (f < 4) are rather unlikely. Therefore, this analysis provides an explanation for why we observe the emergence of fast component only at ~ 20 μW of excitation power corresponding to exciton population of ~20 per SWCNT (FIG. 2 in the main text).

Photon-correlation experiments. Second-order photon-correlation experiments with the gate delay time T_{GD} are based on detection of two emitted photons where the both photons are detected at times larger than T_{GD} after the photoexcitation pulse. Such experiments are typically performed at relatively low pump powers so we can assume that no more than two excitons are present within a single SWCNT at a time. Under these conditions, Eqs. (S1)-(S5) can be used to simulate the results of the second-order photon-correlation experiments. Specifically, the joint probability for two initially created free excitons to emit two photons from trapped states is

$$P_2(T_{GD}) = P_2^{(I)}(T_{GD}) + P_2^{(II)}(T_{GD}), \tag{S16}$$

where

$$P_2^{(I)}(T_{GD}) = \int_0^\infty Q_D k_D dt\, n_5^{(4)}(t) \int_{T_{GD}}^\infty Q_D k_D dt\, n_2^{(1)}(t) \quad , \qquad \text{(S17)}$$

$$P_2^{(II)}(T_{GD}) = \int_0^\infty Q_D k_D dt\, n_5^{(5)}(t) \int_{T_{GD}}^\infty 2Q_D k_D dt\, n_3^{(1)}(t) \quad . \qquad \text{(S18)}$$

Here, $P_2^{(I)}(T_{GD})$ is the joint probability of the sequential emission of two photons in the case where the first photon is emitted by a dopant-trapped exciton *before* the other exciton is trapped; $P_2^{(II)}(T_{GD})$ is the joint probability of the sequential emission of two photons where the first dopant-trapped excitons emits *after* the other exciton is trapped by some other dopant site. The sum of these two probabilities, $P_2(T_{GD})$, can again be found analytically exactly (e.g., in Mathematica) since all $n_i^{(p)}$ can be obtained analytically and then time-integrated. The resulting expression, however, is rather long and cumbersome and consists of a linear combination of time-decaying exponents with various time constants and prefactors. Taking into account that the time resolution is limited by the instrument response function, we discarded all but the slowest-decaying terms in $P_2^{(I)}(T_{GD})$ and $P_2^{(II)}(T_{GD})$, which results in

$$P_2^{(I)}(T_{GD}) \cong Q_D^2 \frac{2m^2 k_t^2 k_D}{k_F(k_F + \alpha k_A - k_t)(k_F + (1-\alpha)k_A + k_t)} e^{-(k_F + \alpha k_A - k_t)T_{GD}} \quad , \qquad \text{(S19)}$$

$$P_2^{(II)}(T_{GD}) \cong Q_D^2 \frac{2m(m-1)k_t^2}{(k_F + \alpha k_A - k_t)(2k_F + k_A)} e^{-2k_D T_{GD}} \quad , \qquad \text{(S20)}$$

where again the realistic assumption $k_D \ll k, k_t, k_A$ was made. These expressions are independent of the EEA-related coefficients η and η' since at most two excitons are considered, so that an EEA event leads to impossibility to detect two photons during a single excitation cycle. In other words, coefficients η and η' can only affect products of EEA, but once EEA occurs, there is no subsequent contribution to $P_2(T_{GD})$.

The time-gated probability for an initially created single free exciton to emit a photon from a trapped state is evaluated similarly

$$P_1(T_{GD}) = \int_{T_{GD}}^{\infty} Q_D k_D dt\, n_5^{(4)}(t) \cong Q_D \frac{m k_t}{k_F} e^{-k_D T_{GD}} \quad . \tag{S21}$$

Conventional normalization of the central-to-side peak ratio in the photon correlation experiment is evaluated as[10]

$$R(T_{GD}) = \frac{\langle n(n-1)\rangle}{\langle n\rangle^2} = \frac{\sum_n n(n-1) p_n P_n(T_{GD})}{\left[\sum_n n p_n P_n(T_{GD})\right]^2} \quad . \tag{S22}$$

where Poissonian probabilities p_n were defined above. At low pump powers the relevant probabilities become $p_1 \cong f$ and $p_2 \cong \frac{f^2}{2} \ll p_1$, which results in

$$R(T_{GD}) \cong \frac{P_2(T_{GD})}{P_1^2(T_{GD})}, \tag{S23}$$

Substituting Eqs. (S15), (S18), (S19) and (S20) into this expression we finally obtain

$$R(T_{GD}) \cong \frac{k_F}{k_F + \alpha k_A - k_t}\left[\frac{m-1}{m}\frac{2k_F}{2k_F + k_A} + \frac{2k_D}{k_F + (1-\alpha)k_A + k_t} e^{-(k_F + \alpha k_A - k_t)T_{GD}}\right]. \tag{S24}$$

1. S. Berciaud, L. Cognet, and B. Lounis, *Phys. Rev. Lett.*, 2008, **101,** 077402.
2. L. Oudjedi, A. N. G. Parra-Vasquez, A. G. Godin, L. Cognet, and B. Lounis, J. *Phys. Chem. Lett.*, 2013, **4,** 1460.
3. J. J. Crochet, et al., *Nano Lett.,* 2012, **12,** 5091.
4. X. Ma, et al., *Phys. Rev. Lett.*, 2015, **115,** 017401.
5. F. Wang, et al.,. *Phys. Rev. B,* 2006, **73**, 245424.
6. N. F. Hartmann, et al., *ACS Nano*, 2016, **10,** 8355.
7. S. M. Santos, et al., *Phys. Rev. Lett.,* 2011, **107,** 187401.
8. M. Kim, et al., *J. Phys. Chem. C,* 2016, **120,** 11268.
9. T. Hertel, et al., *ACS Nano,* 2010, **4,** 7161.
10. G. J. Nair, J. Zhao, and M.G. Bawendi, *Nano Lett.,* 2011, **11,** 1136.